

Determination of position and radius of ball joints

Marjolein van der Glas^a, Frans M. Vos^{ab}, Charl P. Botha^c, and Albert M. Vossepoel^a

^aPattern Recognition Group, Delft University of Technology,
Lorentzweg 1, 2628 JC Delft, the Netherlands

^bDepartment of Radiology, Academic Medical Center, Amsterdam

^cComputer Graphics and CAD/CAM Group, Delft University of Technology,
Mekelweg 4, 2628 CD Delft, the Netherlands

ABSTRACT

For successful ball-joint replacement surgery, it is important to maintain the joint's geometric center. Pre-operative detection of this center is achieved by detecting the sphere that fits onto the articular surfaces in CT or MRI images. We have developed a novel technique to automatically determine the sub-voxel position and size of a sphere in unsegmented 3D images. The method is invariant to size and robust to noise. It only needs one fourth of a sphere to detect the center. Isotropically as well as anisotropically sampled images can be used. As no segmentation is required, it can be applied directly to clinical images.

Keywords: Hough transform, sphere detection, ball joint, CT, MRI

1. PURPOSE

In recent years, biomedical and technological advances have allowed the success rate for replacement of ball joints, such as the hip, to reach levels as high as 90%.¹ Unfortunately, shoulder replacements have failed to reach these levels. Reasons for this are the complex anatomy of the shoulder and the limited industrial interest.

During a total shoulder replacement the glenohumeral joint connecting the humerus and the scapula, is substituted by a prosthesis (figure 1). Most important for successful surgery is that the center of rotation of the glenohumeral joint is maintained.² The joint is a loose ball-and-socket joint, in which the humeral head is the ball and the glenoid is the socket. During motion, the two geometric centers of both spherical surfaces coincide in the center of rotation of the glenohumeral joint.² Thus, the problem of finding this center can be reduced to finding the center of a sphere.

In this paper we present a novel Hough-based technique to automatically determine the center and size of a sphere in unsegmented 3D images, using the direction and strength of the gradient. A fitting method³ would fit a sphere onto the entire top of the humerus instead of onto the articular surface only. In the next section the method is explained. It is tested on artificial images of spheres and used to determine the center of the humeral head in 3D images generated by CT and MRI. Section 3 shows the results of these experiments.

2. METHODS

The Hough transform⁴ is a well accepted method used for shape detection in binary images. Generally, it employs segmented images to determine the parameters of pre-defined shapes. The novelty in our approach is the possibility to use grey-value images.

Consider a parameterization of a sphere by the position of its center (x_0, y_0, z_0) and its radius r . Similar to the implementation for circles suggested by Mc Laughlin,⁵ sphere detection is organized into two stages. First, the sphere center is determined, and next the radius.

Author e-mail: {marjolein,frans,albert}@ph.tn.tudelft.nl, c.p.botha@its.tudelft.nl

Send correspondence to A.M. Vossepoel.

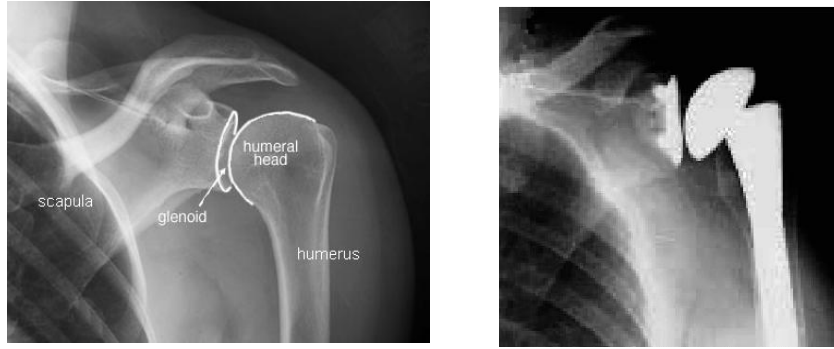


Figure 1: X-ray of glenohumeral joint: healthy (left), with prosthesis (right).

Center detection

To detect the center of a sphere in a 3D image, note that for all voxels on a sphere in a 3D image, the corresponding center will lie on the normal to any local isosurface. The normal of the isosurface through a voxel is defined by the gradient vector. To provide continuous derivatives of discrete data, we use Gaussian derivatives to calculate these vectors. Similar to a Hough transform, a 3D parameter space is defined, containing a probability count for all possible sphere centers. The parameter space is filled by going through the following steps for every voxel in the grey-value image:

1. Determine the orientation and magnitude of the gradient, using Gaussian derivatives.
2. Project the gradient vector in parameter space using Bresenham's line algorithm.⁶
3. Increase the count of the corresponding voxels in parameter space by the gradient magnitude.

The maximum in the parameter space corresponds with the center of the sphere. Three second order polynomials are fitted on the maximum count and its 6-connected neighbours in parameter space to obtain sub-voxel precision. The maxima of these polynomials represent the coordinate of the center on sub-voxel level in x, y and z-direction.

CT and MRI do not always produce isotropic voxels, causing spheres to become ellipsoids. Fortunately, the rate of anisotropy is generally known in advance (slice thickness versus in-plane voxel size). In our method, the anisotropy is taken into account by scaling Bresenham's line algorithm.

Determination of the radius

The radius is determined using a plot of the gradient strength per radius calculated from the detected sphere center, called a radial histogram. To that end, the sum of the gradient magnitudes of all voxels with equal distance to the center is determined. Maxima in the histogram correspond with the radius of the sphere.

3. RESULTS

We performed experiments in which we varied the following parameters in combination with the signal to noise ratio (SNR):

Sphere size Because the radius of the humeral head varies per person.

Sphere fraction Because the humeral head is not a complete sphere.

Anisotropy in z-direction Because CT and MRI do not always produce isotropic voxels.

Parameter Space Because its size and resolution can be varied at will.

The radius of the humeral head typically ranges from 19 mm for a small female up to 28 mm for a large male.⁷ In clinical images, with a typical voxel size of 0.7^3mm^3 , the corresponding radius is between 27 and 40 voxels. The part of the surface of the humeral head that is spherical covers about 4 steradian, or 30% of a total sphere.

Table 1. Inaccuracy, i.e. distance between the determined and the real sphere center, in voxels, for various radii (vertically) and signal-to-noise-ratio of Gaussian noise (horizontally) determined with the optimal sigma (*between brackets*) for solid complete spheres.

R	no noise	40 dB	28 dB	16 dB	9 dB	4 dB	0 dB
26.00	0.112 (1.0)	0.086 (1.5)	0.074 (2.0)	0.073 (3.0)	0.085 (4.5)	0.109 (6.0)	0.097 (5.0)
28.00	0.103 (1.0)	0.071 (1.5)	0.081 (2.0)	0.079 (3.0)	0.076 (3.5)	0.100 (5.5)	0.096 (7.5)
30.00	0.099 (1.0)	0.066 (1.5)	0.074 (2.0)	0.068 (3.5)	0.077 (5.0)	0.095 (6.5)	0.081 (6.0)
32.00	0.094 (1.0)	0.066 (1.5)	0.062 (2.0)	0.077 (3.0)	0.076 (4.0)	0.085 (4.5)	0.101 (6.5)
34.00	0.086 (1.0)	0.064 (1.5)	0.054 (2.0)	0.079 (3.5)	0.090 (5.5)	0.091 (5.0)	0.104 (6.0)
36.00	0.093 (1.0)	0.074 (1.5)	0.065 (2.0)	0.077 (4.0)	0.088 (5.0)	0.065 (6.0)	0.112 (6.0)
38.00	0.099 (1.0)	0.071 (1.5)	0.067 (2.0)	0.071 (3.5)	0.076 (6.0)	0.089 (6.5)	0.127 (8.5)
40.00	0.085 (1.0)	0.056 (1.5)	0.059 (2.0)	0.086 (4.0)	0.090 (5.5)	0.082 (9.5)	0.139 (8.0)

Properties of CT and MRI images

In our MR images the grey-values of the voxels range from 0 to 512. The lowest grey-values (up to 20) represent bone, grey-values of surrounding tissue are higher. The coefficient of variation of noise measured in bone tissue is 0.2 (SNR=14 dB). The grey-values of CT images ranged from 0 to 2700. Cortical bone has a mean grey-value of 2000, grey values of surrounding tissue, including trabecular bone, are lower. The outer contour of the bone in the joint is spherical, while the inner contour, the transition from cortical to trabecular bone, is not. Therefore, in CT images, the humeral head is hollow with a smooth but irregular inner boundary and a sharp outer boundary. The signal to noise ratio of the image is about 28 dB.

Properties of artificial images

The method is validated using artificial images. Images are created with one solid sphere, its edge is blurred by a Gaussian blur with sigma 1. By default an image contains a complete sphere with a radius of 34 (average size of a humeral head at a resolution of $0.7^3 mm^3$). The image is isotropically sampled. The voxel sizes in parameter space and in the artificial image are chosen equal. The size of the parameter space is 21^3 voxels. This size can be varied at will. The more accurate the first estimation of the center position is, the smaller the parameter space may be.

To cover a broad range of noise-levels, the artificial images Gaussian noise is added to the images with the coefficient of variation of noise varying from 0 to 1 (no noise to a SNR of 0 dB). For each measured combination of parameters 20 artificial images were generated, in which the sub-voxel center position of the sphere is varied. For each image, the center position, optimal sigma and radius are determined. The ‘optimal sigma’ is the sigma of the Gaussian derivative for which the inaccuracy of the center detection is minimal.

Sphere size, sphere fraction and anisotropy in z-direction

Table 1 shows the average distance between the real and determined sphere center, determined using the optimal sigma. It can be seen that the average error in the center detection is less than 0.1 voxel. The optimal sigma increases for decreasing SNR, and for increasing size of the sphere.

The surface fraction is defined as the surface of the part of the sphere inside the image divided by the surface of the complete sphere. The result of varying the surface fraction is shown in figure 2. As expected, the determination of the sphere center becomes less robust to noise for smaller surface fractions. The optimal sigma is not changed by changing surface fraction. As the spherical part of humeral head covers about 30% of a sphere, the expected inaccuracy in clinical images is 0.1 voxel.

CT and MRI do not always produce isotropic voxels. Figure 3 shows the error in center detection for the optimal sigma and for different ‘elongation’ in z-direction. Anisotropically sampled images are less robust to noise than isotropically sampled images. As clinical images contain little noise, known anisotropy will have little effect on the accuracy of position of the center of the humeral head. The optimal sigma is only affected by variation in noise level, not by variation in elongation.

Computation time and parameter space

For images of 84^3 voxels, computation time is 3.5s on a 700MHz Dual Pentium Processor with 2 GB internal memory. Computation time can be reduced by only recording the normals in a small area around a first estimate of the sphere center. If the real center is within this area, the accuracy of the center detection will not be affected.

In previous experiments, the discretization of the parameter space is done in such a way that the size of a voxel, v_s , in the parameter space is equal to one in the artificial image. Varying the size of a voxel in parameter space inversely affects both computation time and accuracy. Figure 3 shows the inaccuracy of the center position, expressed in voxels of the input image, for decreased as well as increased voxel size in parameter space. Reducing the voxel size increases the accuracy, but it decreases the robustness to noise. The optimal sigma of the Gaussian derivative decreases for increasing voxel size. Figure 4 shows that computation time exponentially increases for decreasing voxel size in parameter space.

Accuracy of the radius determination

The determination of the radius is affected by the sigma of the Gaussian derivative, as this introduces smoothing. Smoothing increases the size of the sphere, as the new outer boundary has a larger perimeter. When the gradient magnitude is determined using a Gaussian derivative with a sigma of 1, the measured radius is found to be 0.78 voxel larger than the real radius for a perfect positioning of the center.

In figure 5 the effect of noise and deliberate inaccuracy of the center positions on the radius measurements is shown. For small inaccuracy of the center position, the determination of size is robust to noise.

Clinical images

In clinical MRI and CT images of the glenohumeral joint, the center position and the radius of the approximate sphere are determined. In MR images the center is determined using a sigma value 3.5, which is optimal for a signal-to-noise-ratio of 14 dB. In the radial histogram two peaks show up, the first peak is caused by the humeral head and the second one by the glenoid. A slice of the scan, with both sphere and the determined center is shown in figure 6.

Figure 6 also shows the result of the center detection and radius determination of the humeral head in a CT image. As CT generally produces images with less noise than MRI, the used sigma value is 1.5. Although a radius can be determined for the glenoid, the bone surface of the glenoid is too flat to give a reliable spherical match. Therefore only one sphere is drawn.

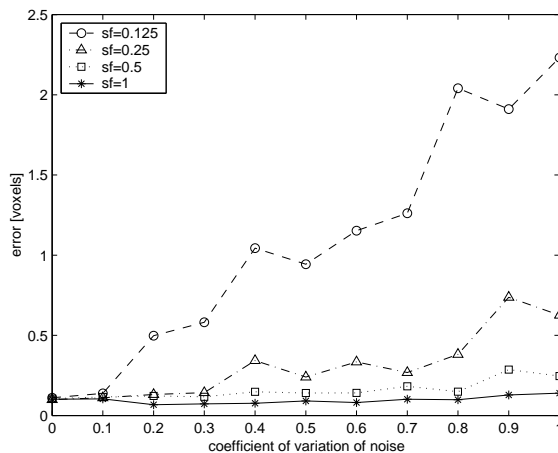


Figure 2: Inaccuracy of the center position versus the coefficient of variation for different surface fractions, sf .

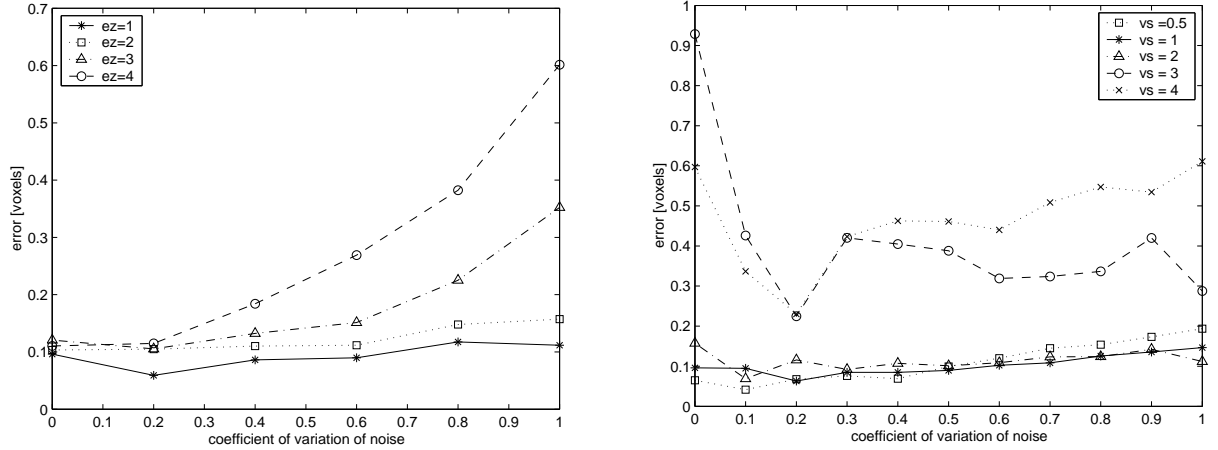


Figure 3. Error in center detection versus the coefficient of variation of noise for anisotropy in z-direction, ez (left). Position inaccuracy of the sphere center as function of the coefficient of variation for various voxel sizes, vs , in the parameter space (right).

4. CONCLUSION

The Hough-based method can detect the center position of a sphere with an inaccuracy of less than 0.1 voxel. This detection is invariant to the size of the sphere. For images containing at least 50% of the surface of a sphere, the method is robust to noise up to a SNR of 1 dB. For smaller surface ratios, the error increases for low SNR (lower than 40 dB for 12.5%, 10 dB for 25%). Anisotropic sampling of the image decreases the robustness to noise. In clinical images, the elongation in z-direction is normally less than 3. As the coefficient of noise in these images is lower than 0.3 and the typical surface ratio of the humeral head is 30%, known anisotropy will not affect the accuracy of the detection of the center of the humeral head.

In all experiments the ‘optimal sigma’ is determined. For images without noise the optimal sigma is 1. For decreasing SNR, the optimal sigma increases. For increasing voxel size in parameter space, the optimal sigma decreases by a factor $1/vs$. Although sigma should be chosen with care, the method is robust to sub-optimally chosen sigmas.

Detection of the center of rotation of the glenohumeral joint can be used in pre-operative planning for shoulder

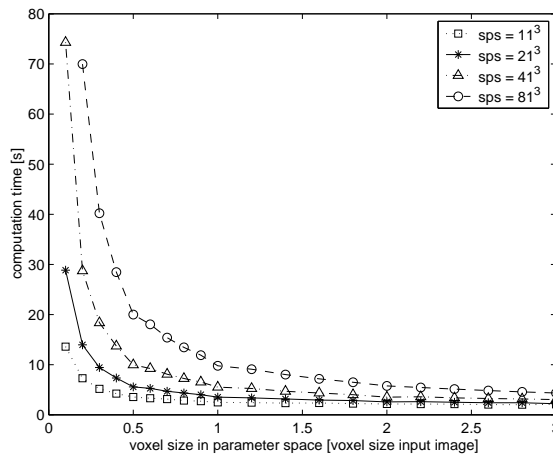


Figure 4. Computation time for image of size 84^3 voxels for various size (sps) of the parameter space, and its voxel size (right).

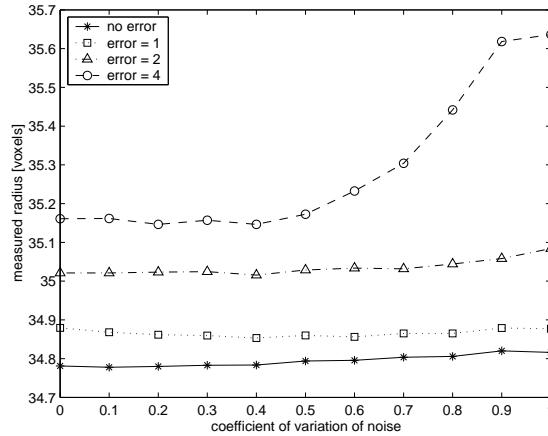


Figure 5: Measured radius versus cv, for various values of the inaccuracy of the center position [voxels]

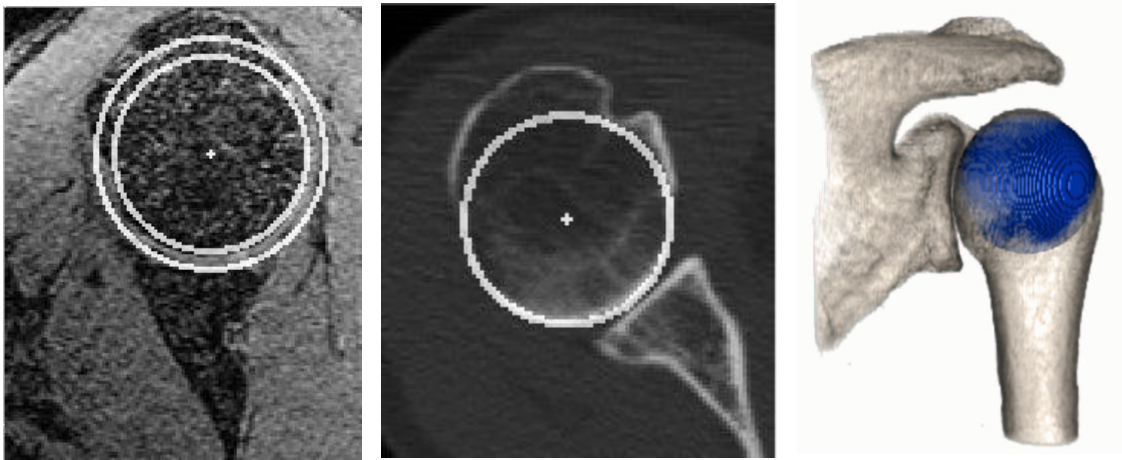


Figure 6. Result sphere detection in MRI (left), in CT (middle), and 3D visualisation of the bone and the detected sphere (right).

replacements. As no segmentation is required, it can be directly applied to clinical images. It will help the surgeon to optimally position the shoulder prosthesis.

ACKNOWLEDGEMENTS

This research is part of the Development of Improved endo-Prostheses for the upper EXtremities (DIPEX) program of the Delft Interfaculty Research Center on Medical Engineering (DIOC-9).

Clinical CT-images were provided by R.E. van Gelder of the Academic Medical Center of Amsterdam. MR-images were provided by M.W. Vogel of the Department of Radiology of the Erasmus University Medical Center.

REFERENCES

1. "Dipex." <http://www.wbmt.tudelft.nl/mms/dipex/>.
2. O. de Leest, M. Rozing, and et al, "Influence of Glenohumeral Prosthesis Geometry and Placement on Shoulder Muscle Forces," *Clinical Orthopedics* **330**, pp. 222–233, 1996.
3. J. Jacq and C. Roux, "Automatic detection of articular surfaces in 3D image through minimal subset random sampling," in *CVRMed-MRCAS'97 proceedings, LNCS 1205*, pp. 73–82, Springer, 1997.

4. V. Leavers, *Shape detection in computer vision using the Hough transform*, Springer Verlag, 1992.
5. R. McLaughlin and M. Alder, "The Hough Transform versus the UpWrite," Tech. Rep. TR97-02, The University of Western Australia, 1997. <http://ciips.ee.uwa.edu.au/ram/papers.html>.
6. J. Foley, A. van Dam, S. Feiner, and J. Hughes, *Computer Graphics, principles and practice*, ch. 3. Addison-Wesley, 1990.
7. J. Iannotti, "The Normal Glenohumeral Relationships," *Journal of Bone and Joint Surgery* **vol. 74-A(4)**, pp. p. 491-500, 1992.